RESEARCH NEWS

Highly Surface-roughened "Flower-like" Silver Nanoparticles for Extremely Sensitive Substrates of Surface-enhanced Raman Scattering

By *Hongyan Liang, Zhipeng Li, Wenzhong Wang, Youshi Wu,* and *Hongxing Xu**

Surface-enhanced Raman scattering (SERS) is a new optical spectroscopic analysis technique with potential for highly sensitive detection of molecules. Recently, many efforts have been made to find SERS substrates with high sensitivity and reproducibility. In this Research News article, we provide a focused review on the synthesis of monodispersed silver particles with a novel, highly roughened, "flower-like" morphology by reducing silver nitrate with ascorbic acid in aqueous solutions. The nanometer-scale surface roughness of the particles can provide several hot spots on a single particle, which significantly increases SERS enhancement. The incident polarization-dependent SERS of individual particles is also studied. Although the different "hot spots" on a single particle can have a strong polarization dependency, the total Raman signals from an individual particle usually have no obvious polarization dependency. Moreover, these flower-like silver particles can be measured by SERS with high enhancement several times, which indicates the high stability of the hot spots. Hence, the flower-like silver particles here can serve as highly sensitive and reproducible SERS substrates.

1. Introduction

Surface-enhanced Raman scattering (SERS) has been intensely researched for many years as a great potential technique for ultra-trace detection.[1] It is generally recognized that two different mechanisms are involved in SERS—one is the chemical enhancement caused by the charge transfer[2] between the

[*] Prof. H. X. Xu, H. Y. Liang, Dr. Z. P. Li, Prof. W. Z. Wang
Institute of Physics
Chinese Academy of Sciences
Beijing, 100190 (P. R. China)
E-mail: hxxu@aphy.iphy.ac.cn
H. Y. Liang, Prof. Y. S. Wu
School of Materials Science and Engineering
Shandong University
Jinan, 250061 (P. R. China)
Prof. W. Z. Wang
College of Science
Minzu University of China
Beijing, 100081 (P. R. China)

molecule and adjacent metal surface, the other is the local electromagnetic enhancement that originates from the excitation of the collective oscillations of free electrons in noble or transition metals such as Ag, Au, Pt, and Ru,[3] where the latter is the main contributor to SERS enhancement, as in most cases it is several orders of magnitude larger than the chemical enhancement. So, based on the local electromagnetic enhancement, by both experiment and theory,[4] three main classes of substrates have been developed to achieve highly sensitive and reproducible SERS measurement: rough surfaces,[5] nanoparticle colloids,[6] and periodic nanostructures.[7] However, it is disappointing that both sensitivity and reproducibility can hardly be found at the same time in any one of these classes. For example, Ag or Au nanoparticle aggregates, 50–100 nm in size, can generate hot spots with very high SERS enhancement (more than 10^{10}), enough even for single-molecule detection.[8] But reproducibility is hardly achieved because each hot spot is small in size and the quality of the SERS enhancement varies.[9] Only through some delicate techniques can the controllable formation of the hot spots in nanoparticles be realized, e.g., by optical forces, atomic force microscopy (AFM)/scanning tunneling microscopy (STM) tips, etc.[10] A rough surface, on the other hand, can provide randomly distributed hot spots over a large area, but usually with lower enhancement (10^2–10^6).[11] Recently, periodic nanostructures have been fabricated by nanometer-scale lithography techniques, and a moderate enhancement (10^5–10^6) has been achieved.[12] But current techniques still have difficulties to set controllable small gaps of a few nanometers between metal nanostructures. Interestingly, the SERS properties of a mesoscopic Au particle with a rough surface are capturing researchers interest.[13] With a spherical shape and roughened morphology, more than a 10^6 SERS enhancement was obtained with a relatively high reproducibility.

We recently performed SERS studies on individual nanometric hole–particle pairs.[14] A single nanoparticle is located in a single nanohole, which creates hot sites between them, thus greatly enhancing Raman signals of probe molecules. The near-parallel

curvatures of the hole edge and the particle surface can make the volume of the hot site much larger than the hot spot located between two spherical particles with opposite curvatures. This new system may have great potential for SERS studies in general, and biosensor applications in particular. We also studied the polarization dependence of SERS in coupled gold nanoparticle–nanowire systems.[15] The coupling between the continuous nanowire plasmons and the localized nanoparticle plasmons gives significant field and SERS enhancements comparable to those found in nanoparticle dimer junctions. We also found that only the part of local intensity enhancement ($E^2(\theta, \omega)$) in the total SERS enhancement is dependent on the incident polarization, while the part of Raman emission enhancement at the Raman frequency ω_R will be fixed at about the maximum value of the local intensity enhancement $|E^2(\theta, \omega_R)|_{max}$, and is not polarization independent. This part of Raman emission enhancement is determined by the nanoantenna effect of the metal nanostructure itself only. When the molecule position and the metal nanostructure are fixed, this part of SERS enhancement will be fixed. In multiparticle systems, it has been found that the antenna effects can tune the emitted polarization of SERS, which could be used for the design of polarization nanorotators.[16,17]

In this Research News article we provide a focused review of the synthesis of flower-like Ag particles with sizes from 500 nm to 2 μm. The Ag particles have highly roughened surfaces with a roughness of 30–100 nm depending on the particle size, which could provide vast hot spots over the whole particle surface. It is found that the Raman scattering of molecules adsorbed on a single Ag particle surface can be enhanced by about 7–8 orders on average. For malachite green isothiocyanate (MGITC) molecules, at concentrations down to 10^{-10} M, Raman signals can still be clearly observed from most of the individual Ag particles. The incident polarization dependency of the Raman signal from the hot spot on the surface of the particle further reveals that the high enhancement originates from the local coupling of nanometer-scale protrusions and crevices on the randomly textured surface.

2. Highly Surface-roughened Flower-like Silver Nanoparticles

In a typical synthesis, a AgNO₃ aqueous solution (0.2 mL, 1 M) and a poly(vinyl pyrrolidone) (PVP, $M_w \approx 40\,000$, 2 mL, 0.1 M) aqueous solution were added to deionized water (10 mL) in a beaker with a magnetic stirrer at room temperature. The concentration of PVP was calculated in terms of the repeating units. An ascorbic acid (AA, $C_6H_8O_6$, 0.2 mL, 1 M) aqueous solution was then quickly
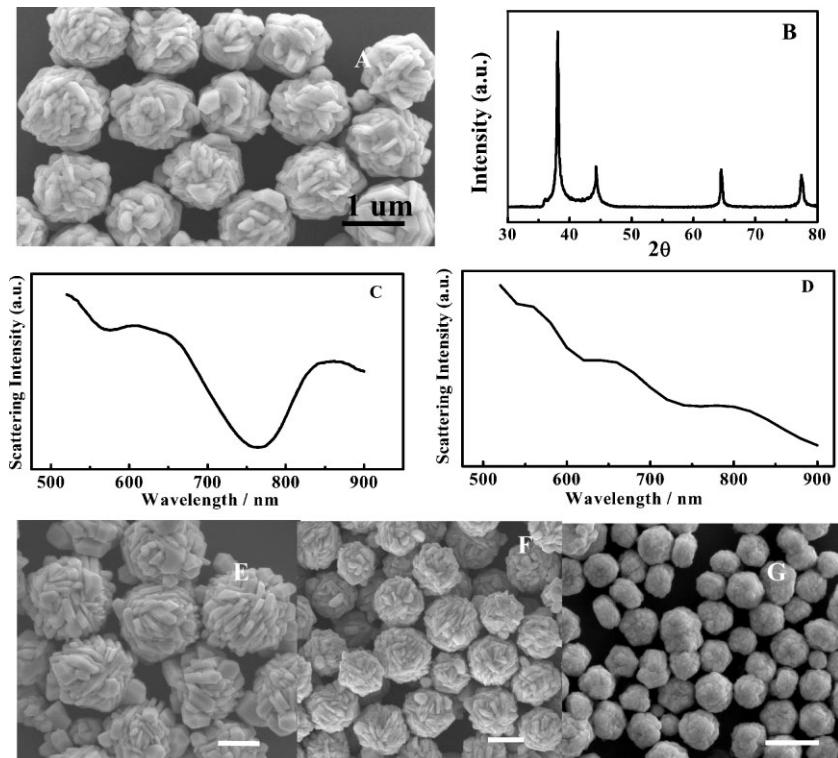

Figure 1. A) SEM image of flower-like silver particles. B) XRD pattern taken from the same batch of sample. C) DF scattering spectrum of a single particle. D) Theoretically calculated scattering spectrum of an Ag sphere with the same size as in the experiment. The multipoles in the simulation is taken up to 40, which is enough for the convergence of the simulation. E–G) SEM images of flower-like Ag particles with different sizes obtained by changing the concentration of silver nitrate in reacting solution. E) 100×10^{-3} M, F) 20×10^{-3} M, and G) 4×10^{-3} M. All scale bars are 1000 nm.

injected into the vigorously stirred mixture. The solution became grey immediately and then changed to dark grey a few minutes later, which indicated the appearance of a large quantity of colloidal silver particles. A sample of the silver particles was obtained by centrifugation and was washed with ethanol several times in order to remove the excess surfactant. By this procedure, colloidal silver nanoflowers with a radius of about 700 nm can be obtained. By changing the concentration of silver nitrate in the reacting solution from 0.04 to 0.1 M (diluted by deionized water only), the particle size could be tuned from 500 nm to 2 μm in diameter, with examples as shown in Figure 1E–G.

The morphology of these particles was investigated by scanning electron microscopy (SEM) with typical images of the particles shown in Figure 1A. These particles have a spherical profile, but with a highly roughened surface, which consists of many irregular and randomly arranged protrusions (30–100 nm). Deep crevices (tens of nanometers) were naturally formed between these protrusions. The crystal structure and the phase composition of these particles were characterized by X-ray diffraction (XRD). Figure 1B shows a typical XRD pattern of the as-prepared product. Four peaks can be observed, which correspond to diffractions from the (111), (200), (220), and (311) planes of the face-centered-cubic (fcc) phase. This indicates that the flower-like Ag particles are well crystallized.

The optical properties of individual flower-like Ag particles were investigated by dark field (DF) spectroscopy. The DF scattering spectra were measured with a Renishaw in Via micro Raman spectroscopy system. The sample was illuminated by unpolarized white light from a 100 W halogen lamp through a DF condenser (NA = 1.4–1.2). The DF scattered light was obtained through a ×50 objective (NA = 0.75). Figure 1C shows a typical DF scattering spectrum measured from a single particle with a diameter of about 1 μm. Two peaks at about 610 and 870 nm in the DF spectrum correspond to the quadrupolar and dipolar scattering, respectively, while the higher modes are suppressed because of the very rough surface of the particle.[13] The scattering spectrum of a spherical particle (1 μm in diameter) with a perfectly smooth surface is calculated using Mie scattering theory[18] as shown in Figure 1D. The main features of quadrupolar and dipolar scattering appear at 630 and 810 nm, respectively, which are quite close to the experimental data. The differences in resonance frequencies and spectroscopic line shapes between the experiment and simulation are probably caused by the presence of nanometer-scale roughness on the particle surface in the experiment, while roughness was not represented in the simulation.

Figure 2. Optical microscopy (A) and SEM (B) images of the same flower-like silver particles. The scale bar in (B) is 10 μm. C) The normal Raman spectrum of the pure MGITC powder. D) The Raman spectra from individual bare silver particles without MGITC molecules. E) SERS spectra from different single flower-like silver particles marked as I–V in (A). All spectra were measured with the same accumulation time (60 s), and with 200 counts per division in (D) and (E) and 10 000 counts per division in (C).

3. Applications in SERS Substrates

3.1. Extremely High SERS on a Single Flower-like Particle

The SERS sensitivity of these flower-like silver particles was tested using MGITC molecules. MGITC can bind strongly to the silver surface by the sulfur atom of its isothiocyanate group, and the resonance of MGITC is close to the excitation wavelength at 632.8 nm used here. Samples for SERS measurements were prepared by the following processes: 0.1 mL of an ethanolic MGITC solution (10^{-10} M) was mixed with the same volume of a Ag colloidal solution for 24 h in order to achieve a high adsorption of MGITC molecules. Eighty percent of the molecules are estimated to adsorb onto the Ag nanoparticles. The corresponding concentration of the flower-like Ag particles in the colloidal solution is estimated to be about 10^{-12} M. A droplet of such an incubated mixture was then spin-coated on a clean Si substrate, and then rinsed with ethanol to remove any free molecules in the solution. Well-separated individual particles were observed on the Si substrate. Figure 2A shows an optical image of the Ag particles, and the corresponding SEM image is shown in Figure 2B. With the help of a transmission electron microscopy (TEM) grid, each isolated single particle can be clearly identified in both the optical and SEM images as marked I–V.

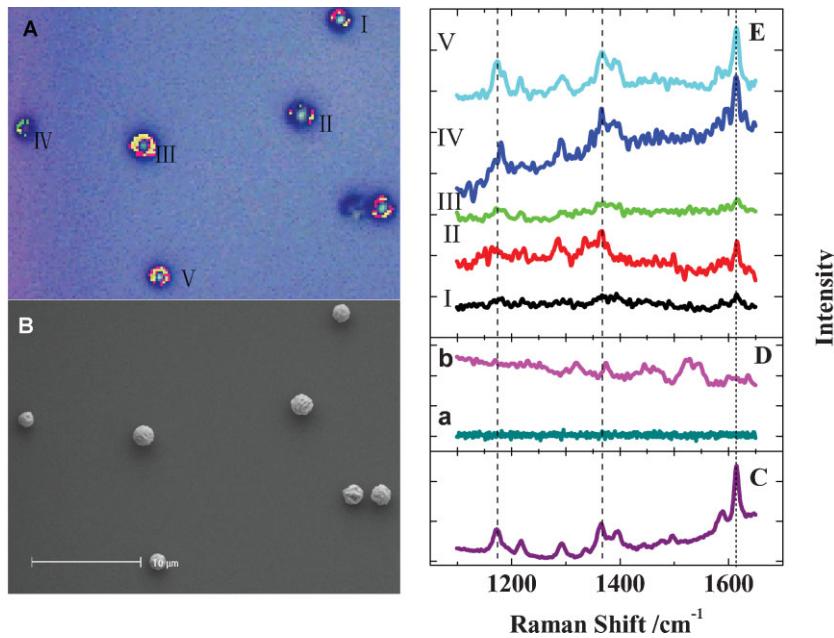The SERS spectra were collected by the same Raman spectroscopy system as mentioned above with a 632.8 nm HeNe laser as the excitation source. This excitation wavelength is very close to the scattering resonance at 610 nm as shown in Figure 1C. The laser beam was focused on the samples through a ×50 objective and Raman signals were collected through the same objective in the backscattering geometry. An extremely low incident laser power (in the μW range) was used in order to minimize heating and photochemical effects during SERS measurements and the acquisition time was 60 s. Figure 2C shows the normal Raman spectrum of the pure MGITC powder. Figure 2D shows Raman spectra from individual bare silver particles without MGITC molecules. Since most of the pure silver particles surface was clean after washing several times, no noticeable Raman signals can be observed. Such a typical Raman spectrum is shown in Figure 2Da. Occasionally, some individual particles give Raman signals, probably caused by amorphous carbon as shown in Figure 2Db, but it would not affect the SERS detection of MGITC molecules because the positions and intensities of all Raman peaks are arbitrary for different particles.

Figure 2E shows the Raman spectra from single particles I–V as marked in Figure 2A, which clearly show the main vibrational features of MGITC molecules: the positions and relative intensities of three peaks at 1173, 1365, and 1615 cm^{-1} are similar to a normal SERS spectrum as in Figure 2C. It should be noted that these five particles are randomly chosen, and detectable SERS signals can be acquired in each single particle. Most other individual particles investigated under the same experimental conditions can give quite strong SERS signals of MGITC molecules, and the average relative standard deviation of the intensities of these three peaks is less than 10%, which shows

that the reproducibility and stability of these flower-like silver nanostructures make them suitable for highly sensitive SERS substrates. SERS enhancement factors can be calculated by comparing the ratios of the peak intensities of MGITC molecules on a single particle to the corresponding un-enhanced signals from a crystal-like powder, and the enhancement factors were estimated to be on the order of 10^7–10^8. This result is nearly one order of magnitude higher than the SERS enhancement from the Au meatball particles reported previously.[13] Furthermore, these enhancement factors are the average enhancements over the whole surface of each particle, and highly localized SERS enhancements on the tips of the protrusions or inside the crevices on the surface of each particle should be significantly larger. The SERS enhancement factors of close-packed arrays of Ag nanoflowers were also estimated in a similar way to be approximately 50 times larger than individual particles. Such increases in SERS enhancement arizes from the additional field enhancements in the interparticle gaps.[8,19]

Figure 3. A) The Raman images of a single Ag nanoflower for different incident polarizations. The arrows show the different polarizations. B) The corresponding SEM image of a single particle. C) Polar plots of the Raman intensities of spot I and II marked in (A). D) Polar plots of total Raman intensity from the whole particle. All scale bars are 1 μm.

3.2. Incident Polarization-dependent SERS of Individual Particles

Raman imaging can show the spatial distribution of SERS enhancement on the surface of silver particles, which may provide a more fundamental understanding of such high SERS enhancement on a single particle. The measurement of the Raman image is performed using the TE air cooled 576 × 400 CCD array in a confocal Raman system at the Raman shift of 1615 cm^{-1} with a spectroscopic window width of ± 20 cm^{-1}, while the laser light was blocked by a 633 nm edge filter. The objective used in the measurement is ×100 (NA = 0.95). The SEM image in Figure 3B shows the detailed topography of the investigated particle with a diameter of 2 μm. Because of the large surface area, different well-separated hot spots on the particle could be distinguished clearly. Owing to the texture of the nanostructures at the surface of the silver particles, it is not surprising that multiple hot spots can co-exist on one particle. Figure 3A shows polarization dependency measurements for the particle shown in Figure 3B. The polarization direction of the incident laser was tuned by a half wave plate and the efficiency of the Raman system at different polarizations was corrected. It is clear that two bright spots marked as I and II in Figure 3A have different polarization dependencies. Polar plots of Raman intensities for these two hot spots at different polarization angles are shown in Figure 3C. The favorite polarization angles for the maximum intensities of these two hot spots differ by 60 degrees. However, the total SERS intensity of the whole particle did not show obvious polarization dependence. Polar plots in Figure 3D show the intensity variation of the whole particle. Except for the decay of the Raman intensity, which is probably a result of the
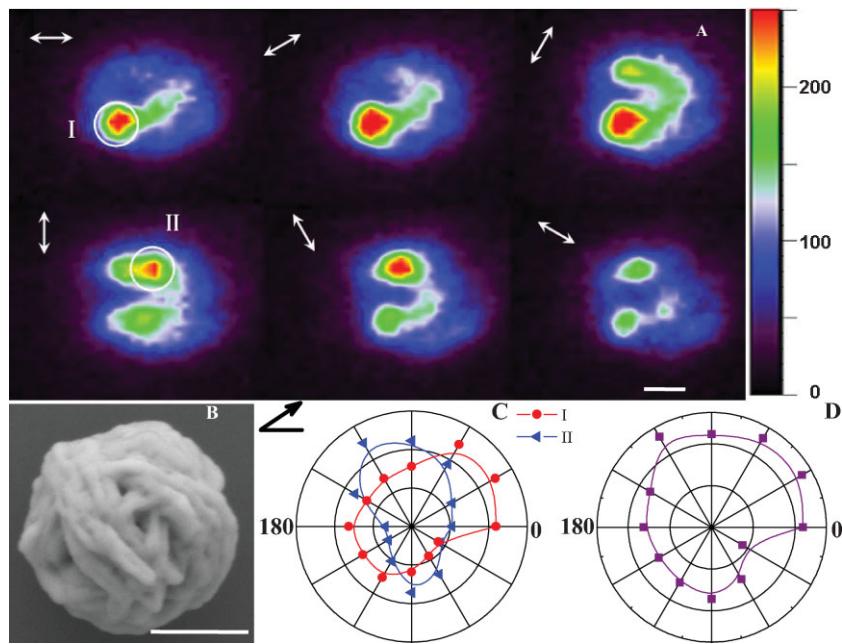
degradation of MGITC molecules under an enhanced local field, the SERS signals would not show much polarization dependency. Other flower-like silver particles that have been investigated have very similar polarization dependent behaviors. Since the favorite polarization directions of hot spots are random, the total contribution to the polarization from multiple hot spots on one particle can be isotropic. This feature is actually an advantage for the flower-like silver particles as highly sensitive SERS substrates, since no certain incident polarization is required.

4. Conclusions

In conclusion, flower-like silver particles with a nanometer-scale roughness on their surfaces have quite high and reproducible SERS enhancements in the order of 10^7–10^8 on average. Owing to the textured nanostructures at the surface of the silver particles, there are multiple hot spots with different polarization dependencies for SERS on one particle, and the total contribution to the polarization dependency of SERS from multiple hot spots on one particle can be isotropic. The flower-like silver particles may have many advantages as highly sensitive SERS substrates. For example, these flower-like silver nanoparticles are very stable and can be reused several times as SERS substrates. In an aqueous environment, silver nanoflowers can be stored for more than one year without obvious deterioration, and the highly sensitive SERS characteristics remain. In comparison with aggregates of small particles of less than 100 nm, multiple hot spots in our system are easily located on a single particle, which benefits SERS for trace analyses. Moreover, these particles are very easy to synthesize rapidly on a large scale, and no by-products

RESEARCH NEWS

will pollute the environment. Hence, the flower-like silver particles investigated here could be promising candidates for SERS.

Acknowledgements

[1] M. Moskovits, *Top. Appl. Phys.* **2006**, *103*, 1.

[2] M. Sun, S. Wan, Y. Liu, Y. Jia, H. Xu, *J. Raman Spectrosc.* **2008**, *39*, 402.

[3] (a) H. H. Raether, *Surface Plasmons*, Springer, Berlin **1988**. (b) Z. Q. Tian, B. Ren, D. Y. Wu, *J. Phys. Chem. B* **2002**, *106*, 9463.

[4] (a) K. Zhao, H. X. Xu, B. H. Gu, Z. Y. Zhang, *J. Chem. Phys.* **2006**, *125*, 81 102. (b) H. Wang, C. S. Levin, N. J. Halas, *J. Am. Chem. Soc.* **2005**, *127*, 14 992. (c) Y. G. Sun, G. P. Wiederrecht, *Small* **2007**, *3*, 1964. (d) Z. Q. Tian, B. Ren, J. F. Li, Z. L. Yang, *Chem. Commun.* **2007**, *34*, 3514.

[5] M. Fleischmann, P. J. Hendra, A. J. McQuillan, *Chem. Phy. Lett.* **1974**, *26*, 163.

[6] (a) H. X. Xu, J. Aizpurua, M. Käll, P. Apell, *Phys. Rev. E* **2000**, *62*, 4318. (b) F. Le, D. W. Brandl, Y. A. Urzhumov, H. Wang, J. Kundu, N. J. Halas, J. Aizpurua, P. Nordlander, *ACS Nano* **2008**, *2*, 707.

[7] (a) L. Gunnarsson, E. J. Bjerneld, H. Xu, S. Petronis, B. Kasemo, M. Kall, *Appl. Phys. Lett.* **2001**, *78*, 802. (b) S. J. Lee, Z. Q. Guan, H. X. Xu, M. Moskovits, *J. Phys. Chem. C* **2007**, *111*, 17 985.

[8] (a) H. X. Xu, E. J. Bjerneld, M. Käll, L. Börjesson, *Phys. Rev. Lett.* **1999**, *83*, 4357. (b) A. M. Michaels, J. Jiang, L. Brus, *J. Phys. Chem. B* **2000**, *104*, 11 965.

[9] S. E. J. Bell, N. M. S. Sirimuthu, *Chem. Soc. Rev.* **2008**, *37*, 1012.

[10] (a) F. Svedberg, Z. P. Li, H. X. Xu, M. käll, *Nano Lett.* **2006**, *6*, 2639. (b) L. M. Tong, Z. P. Li, T. Zhu, H. X. Xu, Z. F. Liu, *J. Phys. Chem. C* **2008**, *112*, 7119. (c) J. H. Tian, B. Liu, X. L. Li, Z. L. Yang, B. Ren, S. T. Wu, N. J. Tao, Z. Q. Tian, *J. Am. Chem. Soc.* **2006**, *128*, 14 748.

[11] M. F. Mrozek, D. Zhang, D. Ben-Amotz, *Carbohydr. Res.* **2004**, *339*, 141.

[12] C. L. Haynes, A. D. McFarland, R. P. Van Duyne, *Anal. Chem.* **2005**, *77*, 338A.

[13] H. Wang, N. J. Halas, *Adv. Mater.* **2008**, *20*, 820.

[14] H. Wei, U. Hakanson, Z. L. Yang, F. Hook, H. X. Xu, *Small* **2008**, *4*, 1296.

[15] H. Wei, F. Hao, Y. Z. Huang, W. Z. Wang, P. Nordlander, H. X. Xu, *Nano Lett.* **2008**, *8*, 2497.

[16] T. Shegai, Z. P. Li, T. Dadosh, Z. Y. Zhang, H. X. Xu, G. Haran, *PNAS* **2008**, *105*, 16 448.

[17] Z. P. Li, T. Shegai, G. Haran, H. X. Xu, *ACS Nano* **2009**, *3*, 637.

[18] (a) H. X. Xu, *Phys. Lett. A* **2003**, *312*, 411. (b) Z. P. Li, H. X. Xu, J. Quant, *Spectrosc. Radiat. Transfer* **2007**, *103*, 394.

[19] H. X. Xu, J. Aizpurua, M. Käll, P. Apell, *Phys. Rev. E* **2000**, *62*, 4318.